

# In-Silico Investigation of Phytochemicals from the Endemic Libyan Plant *Arbutus pavarii* as Potential COX-2 Inhibitors

Abdelkarim Sasi<sup>\*</sup>, Safa Biauo

Department of Chemistry, Faculty of Pharmacy, University of Misurata, Misurata, Libya

Corresponding Email. [kareem.sasi@gmail.com](mailto:kareem.sasi@gmail.com)

## Abstract

*Arbutus pavarii* Pamp. (Al-Shmari) is an endemic species native to the El-Gabel El-Akhdar region of Libya, characterized by its Mediterranean climate. This plant holds a long-standing tradition of medicinal use for its analgesic and anti-inflammatory effects, yet its comprehensive chemical profile and therapeutic potential remain largely unexplored. To initiate this investigation, a comprehensive data mining of scientific literature was conducted to systematically collect and catalogue phytochemicals from *A. pavarii*. This effort resulted in a dataset of 78 distinct compounds, which were compiled for inclusion in Libya's first Natural Products Database (LibNPDB). Subsequently, advanced chemoinformatic methodologies, including drug-likeness, toxicity predictions, and molecular docking against the cyclooxygenase-2 (COX-2) enzyme, were employed to evaluate the potential anti-inflammatory and analgesic effects of these compounds. The computational analysis revealed that 14 of the 78 compounds exhibit significant inhibitory potential, with predicted binding affinities against the COX-2 enzyme that are comparable or superior to established non-steroidal anti-inflammatory drugs (NSAIDs). These results provide a strong molecular basis that substantiates the plant's traditional use and confirm that compounds from *A. pavarii* represent promising scaffolds for the development of novel analgesic and anti-inflammatory agents. The compounds catalogued in this study have been integrated into the Libyan Natural Products Database (LibNPDB), expanding its content and reinforcing its value as a tool for local and global drug discovery. Furthermore, this research highlights the pharmacological significance of Libya's endemic flora, underscoring the critical need for biodiversity conservation and its potential contributions to health innovation worldwide.

**Keywords:** Phytochemical, Drug Likeness, Drug design, Databases, *Arbutus pavarii*, LibNPDB.

## Introduction

The practice of using plants for healing is a tradition as ancient as human civilization, forming the foundational bedrock of traditional medicine systems across the globe. This vast repository of ethnobotanical knowledge has consistently served as a vital and fertile ground for modern pharmacology. A substantial portion of contemporary pharmaceuticals, including landmark drugs for cancer, infectious diseases, and pain management, are either derived directly from natural products or are synthetic analogues inspired by their complex chemical structures [1]. This long history of using natural products in medicine emphasizes how important it is to continue studying the world's varied flora to find novel therapeutic agents that can solve urgent global health challenges. Chronic inflammation is one of the most prevalent of these challenges; it is a complicated biological reaction that, when dysregulated, plays a major pathogenic role in a variety of severe human illnesses. These include autoimmune disorders such as rheumatoid arthritis, metabolic conditions like type 2 diabetes, cardiovascular diseases, various neurodegenerative disorders, and many forms of cancer [2].

The cyclooxygenase (COX) enzyme, a key mediator in inflammation, exists in two isoforms. The COX-1 isoform is crucial for physiological homeostasis, including gastric protection. In contrast, COX-2 is induced during inflammation, causing pain and swelling, making its selective inhibition a primary therapeutic goal. Current anti-inflammatory drugs, known as NSAIDs, target these enzymes. Traditional NSAIDs like ibuprofen are non-selective and inhibit both COX-1 and COX-2, often causing significant gastrointestinal side effects [3,4]. To address this, selective COX-2 inhibitors were developed, but their use has been associated with an increased risk of cardiovascular events. This therapeutic challenge underscores the urgent need for safer and more effective anti-inflammatory agents. As a result, researchers are increasingly turning to medicinal plants, especially from unique bioregions, as a promising source of novel compounds that may offer improved selectivity and a better safety profile [4-6].

Libya's distinct climate and ecosystems are home to unique flora, including *A. pavarii*, an evergreen shrub endemic to the El-Gabel El-Akhdar region [7]. This plant is deeply embedded in the local culture, where it is recognized by various common and local names. These include "Shmeri" and "Shmar," which are local terms corresponding to the Arabic "Al-Shmari" (الشماري). It is also descriptively called the "Libyan Strawberry tree" ("شجرة الفراولة الليبية") and known by the Arabic name "Al-Qatlab" (القطلب). The endemism of *A. pavarii*, coupled with its local significance, suggests a unique reservoir of novel chemical compounds, shaped by its adaptation to a specific microclimate [8-10]. This distinctiveness has been confirmed by phylogenetic studies. The *Arbutus* genus is known for its rich phytochemistry; for instance, the related *A. unedo* is high in phenolic compounds and flavonoids, which provide significant antioxidant properties [9-11]. The endemic *A. pavarii* is traditionally used in Libyan folk medicine to treat conditions like gastritis and kidney diseases, and its honey is also valued medicinally [12]. Preliminary phytochemical screenings have confirmed the

presence of flavonoids, tannins, triterpenes, and sterols [9-13], identifying compounds such as arbutin, gallic acid, and quercetin [14]. Despite this strong ethnobotanical history, a comprehensive scientific investigation into its specific phytochemical composition and the molecular basis for its therapeutic effects, particularly its anti-inflammatory potential, remains unexplored. This study aims to address this critical knowledge gap.

Validating traditional medicine with conventional experiments is a costly and time-consuming process. Advanced *in-silico* techniques, such as chemoinformatics and molecular docking, provide a rapid, cost-effective solution. These methods analyze compound properties and predict their binding to biological targets, allowing for the swift prioritization of promising candidates [5-6]. This computational approach not only accelerates the identification of high-quality lead compounds but also provides crucial hypotheses to guide and focus subsequent experimental validation, saving significant time, resources, and labor. For instance, a recent study on the flavonoid-rich extracts of *A. pavarii* leaves demonstrated potential anti-fertility effects in male mice, linking the activity to the induction of oxidative stress and spermatogenic arrest, highlighting the potent biological activity of its constituents [11]. Another investigation successfully employed molecular docking to screen phytochemicals from Indian spices, identifying dual inhibitors of both COX and lipoxygenase (LOX) enzymes, which suggests a path toward developing anti-inflammatory agents with broader efficacy and potentially improved safety profiles [15-16]. Similarly, researchers used molecular docking combined with molecular dynamics simulations to predict potent COX-2 inhibitors from the terpenoids of *Zingiber* species, providing detailed insights into their binding mechanisms [17]. These studies underscore the power of *in-silico* methods not only to validate traditional knowledge but also to rapidly identify promising lead compounds from complex natural sources [4-6].

Therefore, the present study was designed to leverage a sophisticated computational workflow to conduct a systematic investigation into the anti-inflammatory and analgesic potential of *A. pavarii*. The primary objectives were threefold: first, to systematically collect and catalogue the known phytochemicals of *A. pavarii* from existing literature, thereby creating a dedicated library to expand and enhance Libya's first Natural Products Database (LibNPDB); second, to perform a comprehensive chemoinformatic analysis of this library to assess the physicochemical and drug-likeness and toxicity prediction of its constituent compounds; and third, to perform molecular docking simulations to evaluate the binding affinities and detailed interaction patterns of these phytochemicals with the active site of the human COX-2 enzyme. By integrating rich ethnobotanical knowledge with modern computational science, this research seeks to provide a robust molecular rationale for the traditional use of *A. pavarii*, identify novel chemical scaffolds for the future development of safer anti-inflammatory drugs, and highlight the critical importance of conserving Libya's unique and invaluable botanical heritage for global health innovation.

## Methods

A library of *A. pavarii* compounds (ArbC) was first compiled from scientific literature, with 2D structures standardized using ChemDraw 13.0. Subsequently, molecular docking simulations were performed in Molecular Operating Environment (MOE) 2013 against the (COX-2) crystal structure, obtained from the Protein Data Bank (PDB ID: 5IKR), and the resulting protein-ligand interaction poses were visualized within the same software [4-6]. Finally, a comprehensive cheminformatics analysis was conducted using Python (version 3.12), leveraging the RDKit and Pandas libraries for data management. This final step involved calculating physicochemical properties, drug-likeness, and the (QED). Toxicity profiles were also predicted using the eToxPred machine learning model [18], and natural product (NP) structural classifications were determined with the NPClassifier deep neural network [19]. All data generated is stored and organized as CSV files.

## Data Mining and Collection Strategy

The search strategy for data collection involved an extensive and systematic approach across multiple sources. A thorough literature review was conducted, focusing on journal articles, theses, and textbooks that documented the extraction of compounds from *A. pavarii*. Key databases such as PubMed, ScienceDirect, Google Scholar and ResearchGate were extensively utilized to identify relevant publications. Additional literature was uncovered through targeted Google searches and by tracing references cited in previously discovered materials, and then all data will be collected and organized in an Excel worksheet [4,7,18]. The development of the data entry tool and database structure was initiated by creating a dedicated "Data" worksheet in Excel. The headers were precisely defined to capture all essential fields; these headers include essential data points such as Compound Name, PubChem CID, SMILES Strings, InChIkey Code, Compound Class, Species Name, Family, Known Uses, Biological Activity, Mode of Action, Source Country, GPS, Collection Date, Authors, and Reference information. All data were linked to at least one referenced source, ensuring that reference information was captured before any other details were added [4,7].

## Ligand Preparation

The first step in molecular docking involves preparing the ligand molecules and seven compounds representing standard NSAID drugs. This process typically begins with obtaining the structural models of the compounds. A comprehensive library of (ArbC) and standard NSAID drugs (Celecoxib, Indomethacin, Mefenamic acid, Diclofenac, Naproxen, Ibuprofen, and Aspirin) will be compiled from various literature sources, chemical databases (e.g., PubChem). For molecular docking, the 2D structures of these compounds will be generated or imported into MOE using their corresponding SMILES. The 3D structures were subsequently generated and subjected to energy minimization using the MMFF94x force field implemented in MOE. Potential ionization states and tautomers relevant at physiological pH (approximated at pH 7.4) were considered and generated within MOE's database or builder tools to account for different possible forms of the ligands. The prepared ligand library was then saved in a suitable format for docking [5,6].

### **Structural Classification**

The structural classification of (ArbC) was accomplished using NPClassifier, which is a deep neural-network-based tool that classifies compounds into a three-tiered hierarchy (Pathway, Superclass, and Class) based on their structural features, which are encoded as molecular fingerprints. To effectively visualize the distribution of dominant chemical structures across each of these three hierarchical categories, pie charts were generated using the Python programming language, providing a clear quantitative representation of the structural diversity within the database [4,19,20].

### **Drug Likeness and Toxicity Prediction**

The drug-likeness and physicochemical properties of the compounds were analyzed using a high-throughput Python script, which computed key descriptors such as SlogP, molecular weight (MW), topological polar surface area (TPSA), rotatable bonds (Rb), and hydrogen bond acceptors (HBA) and donors (HBD) with the RDKit library. Drug-likeness was evaluated against Lipinski's Rule of 5, with violations noted for compounds with MW > 500, SlogP > 5, HBD > 5, or HBA > 10. The distributions of these properties were visualized using charts generated with the Plotly library (version 6.2.0). Furthermore, a toxicity score was predicted for each compound using eToxPred, an Extra Trees Classifier machine-learning model trained on molecular fingerprints. This model provides a binary prediction of general toxicity, where a score of 0.5 or greater indicates a compound is predicted to be "toxic," and has a reported predictive accuracy of approximately 72% [4,19].

### **Protein Preparation**

Protein preparation, a critical first step for molecular docking, began with the COX-2 crystal structure (PDB ID: 5IKR). Using MOE, we selected one protein subunit (A) and prepared it by removing the co-crystallized ligand (mefenamic acid) and other non-essential components. Hydrogen atoms were added, and protonation states were assigned to residues to reflect physiological pH. A brief energy minimization using the MMFF94x force field was then performed to resolve any steric clashes. This process yielded a clean structure of a 3D protein model, which was saved and optimized for the subsequent docking simulations, ensuring a reliable foundation for evaluating ligand interactions [4,5,17].

### **Molecular Docking Protocol**

Molecular docking simulations were conducted using the MOE Dock program with default parameters. The prepared COX-2 protein (PDB: 5IKR) served as the receptor, while a library of 78 (ArbC) and seven standard NSAIDs were docked as ligands. The active site was defined using the coordinates of the co-crystallized mefenamic acid. For each ligand, multiple binding poses were generated and ranked by their free energy of binding ( $\Delta G_b$ ), with the ten most favorable conformations retained for subsequent analysis. The database file generated from the docking procedure was further analysed, with the binding mode (interactions) of the highest ten (10) conformations for each docked molecule in the active site visualized and studied with the help of MOE. A yellow stick rendering was added to the native ligands (Mefenamic acid) obtained from the PDB (5IKR) file, while the (ArbC) were marked in blue stick style for better contrast and to enable the study of the interactions of these docked compounds within the receptor active site. Among the visualizations of the conformation generated from the docking for each molecule, the conformation with the best binding mode (interactions) and the lowest binding energy ( $\Delta G_b$ ) was selected for further analysis [4-6].

### **Accuracy of the docking protocol**

Before docking the (ArbC) the molecular docking (MD) with MOE was performed between the receptors and their native ligand (Mefenamic acid) to validate the docking protocol by calculating the root mean square deviation (RMSD). The RMSD values between the redocked poses and the original poses of the native ligands are indicative of whether the docking protocol is accurate, with values under 2 Å indicative of an accurate protocol. If the RMSD of the best docked conformation of the native ligand is 2.0 Å or less from the experimental one (native ligand), the used scoring function (protocol) is successful [14], [17], [18]. The obtained pose from redocking the native ligands with their receptors was well correlated with the original

poses, with small RMSD values. The ( $\Delta G_b$ ) and the binding mode (interaction) for the native ligands will also be calculated and analysed [5,6,20].

### Statistical Analysis

This study employed descriptive and comparative statistics. Frequencies and percentages were used to analyze the compound library's structural classification and drug-likeness. The docking protocol was validated using Root Mean Square Deviation (RMSD). ( $\Delta G_b$ ) were evaluated using descriptive statistics (median, range) and a comparative analysis, where compounds were ranked against standard NSAIDs, and the median ( $\Delta G_b$ ) of the phytochemical and reference groups was compared.

## Results

### Ligand and Protein Preparation

To establish the framework for the molecular docking study, both the protein target and the ligand libraries were meticulously prepared. The three-dimensional crystal structure of the (COX-2) enzyme was obtained from the Protein Data Bank (PDB ID: 5IKR). This structure was then processed to ensure its suitability for docking simulations, yielding a refined receptor model for subsequent validation and virtual screening. In parallel, a comprehensive ligand library was compiled, which consisted of 78 phytochemicals previously isolated from *A. pavarii* and seven standard NSAID drugs: Celecoxib, Indomethacin, Mefenamic acid, Diclofenac, Naproxen, Ibuprofen, and Aspirin. This dataset is part of the Libya Natural Products Database (LibNPDB) and has been made publicly available for further research at <https://www.libnpdb.ly/libnpdb-search>. This final library, comprising 78 energy-minimized phytochemical structures, was used for the subsequent molecular docking and chemoinformatic analyses [18,21].

### Drug Likeness and Toxicity Prediction

A comprehensive evaluation of the ArbC was conducted to determine its potential as a source for drug discovery. The analysis incorporated key physicochemical parameters, including (MW, SlogP, TPSA, Rb, HBA, and HBD), benchmarked against critical thresholds such as Lipinski's Rule of Five, Veber's rule, and Ghose rule. Notably, as shown in (Figure 1), 71.79% of the compounds met all criteria of Lipinski's rule, reflecting a strong overall alignment with physicochemical properties essential for oral bioavailability. More specifically, high proportions of the compounds conformed individually to the recommended ranges for MW (91.03%), HBA (85.9%), HBD (78.21%), Rb (100%), SlogP (93.59%), and TPSA (74.36%). In addition, 74.35% of the collection satisfied Veber's guideline for oral bioavailability, although only 16.66% fulfilled Ghose's more stringent requirements [5,22].



## Physicochemical Property Comparison



**Figure 1: Physicochemical property analysis of (ArbC). The plots show the distribution of: (a) MW, (b) SlogP, (c) HBD, and (d) HBA. (e) A comparative bar chart illustrating the percentage of compounds in compliance with Lipinski's, Veber's, and Ghose's rules for drug-likeness.**

The Quantitative Estimate of Drug-likeness (QED) provides a continuous score from 0 to 1, where values  $\geq 0.67$  indicate excellent drug-like properties characteristic of marketed oral drugs, scores of 0.4 - 0.67 represent moderate potential, and values  $< 0.4$  suggest poor suitability, with approved drugs averaging  $\sim 0.67$  [25]. The QED scores, calculated and shown in (Table 1), demonstrate that a substantial portion of the (ArbC) library exhibits moderate to high scores, supporting its developmental viability. Complementary Tox Scores from the 'eToxPred' toxicity prediction model reveal that most compounds maintain manageable safety profiles (where a score  $\geq 0.5$  indicates a prediction of toxicity), with isolated higher risk candidates being potentially acceptable in critical therapeutic contexts, such as cancer, where decisions on toxicity are justified by efficacy [18]. These integrated findings establish the library as a promising source of diverse, drug-like natural products for pharmaceutical advancement.

**Table 1: Drug likeness (QED) Score and Tox Score of 78 compounds from *A. pavarii*.**

No	LibNPDB CID	LRO5V*	Veber Rule	Ghose Filter	QED Score*	Tox Score	No	LibNPDB CID	LRO5V*	Veber Rule	Ghose Filter	QED	Tox Score
1	LibNPDB005	0	Pass	Fail	0.45	0.64	40	LibNPDB253	<b>3</b>	Fail	Fail	0.18	0.40
2	LibNPDB008	0	Pass	Fail	0.41	0.89	41	LibNPDB254	<b>2</b>	Fail	Pass	0.28	0.61
3	LibNPDB010	0	Pass	Fail	0.52	0.73	42	LibNPDB255	0	Pass	Pass	0.79	0.43
4	LibNPDB012	0	Pass	Fail	0.45	0.70	43	LibNPDB256	0	Pass	Fail	0.71	0.69
5	LibNPDB015	0	Pass	Fail	0.45	0.82	44	LibNPDB316	0	Pass	Fail	0.65	0.72
6	LibNPDB023	0	Pass	Fail	0.61	0.78	45	LibNPDB317	<b>3</b>	Fail	Fail	0.16	0.46
7	LibNPDB027	0	Pass	Fail	0.62	0.80	46	LibNPDB318	<b>3</b>	Fail	Fail	0.16	0.46
8	LibNPDB039	0	Pass	Fail	0.56	0.57	47	LibNPDB319	<b>3</b>	Fail	Fail	0.16	0.46
9	LibNPDB040	0	Pass	Fail	0.5	0.67	48	LibNPDB320	0	Pass	Fail	0.52	0.54
10	LibNPDB041	0	Pass	Fail	0.44	0.68	49	LibNPDB321	<b>1</b>	Pass	Pass	0.43	0.45
11	LibNPDB063	0	Pass	Fail	0.53	0.69	50	LibNPDB322	0	Pass	Fail	0.62	0.71
12	LibNPDB066	0	Pass	Fail	0.55	0.64	51	LibNPDB324	<b>1</b>	Pass	Fail	0.49	0.69
13	LibNPDB070	0	Pass	Fail	0.55	0.53	52	LibNPDB325	<b>1</b>	Pass	Fail	0.48	0.80
14	LibNPDB072	0	Pass	Fail	0.69	0.56	53	LibNPDB326	0	Pass	Fail	0.66	0.63
15	LibNPDB073	0	Pass	Fail	0.47	0.69	54	LibNPDB327	0	Pass	Fail	0.51	0.61
16	LibNPDB074	0	Pass	Fail	0.72	0.60	55	LibNPDB328	0	Pass	Fail	0.55	0.69
17	LibNPDB077	0	Pass	Fail	0.52	0.57	56	LibNPDB329	0	Pass	Fail	0.56	0.63
18	LibNPDB078	0	Pass	Fail	0.32	0.58	57	LibNPDB330	0	Pass	Fail	0.51	0.66
19	LibNPDB080	0	Pass	Pass	0.63	0.74	58	LibNPDB331	0	Pass	Fail	0.51	0.59
20	LibNPDB090	<b>1</b>	Fail	Fail	0.38	0.49	59	LibNPDB332	0	Pass	Fail	0.57	0.61
21	LibNPDB102	<b>3</b>	Fail	Fail	0.14	0.57	60	LibNPDB333	0	Pass	Fail	0.54	0.69
22	LibNPDB103	0	Fail	Pass	0.3	0.53	61	LibNPDB334	0	Pass	Fail	0.62	0.57
23	LibNPDB109	0	Pass	Pass	0.55	0.77	62	LibNPDB335	0	Pass	Fail	0.72	0.62
24	LibNPDB113	<b>1</b>	Pass	Fail	0.41	0.38	63	LibNPDB337	0	Pass	Fail	0.56	0.58
25	LibNPDB148	0	Pass	Fail	0.45	0.69	64	LibNPDB338	0	Pass	Fail	0.54	0.62
26	LibNPDB165	0	Pass	Fail	0.52	0.70	65	LibNPDB339	0	Pass	Fail	0.62	0.57
27	LibNPDB174	0	Pass	Pass	0.43	0.77	66	LibNPDB350	<b>1</b>	Fail	Fail	0.33	0.50
28	LibNPDB187	0	Fail	Pass	0.22	0.68	67	LibNPDB351	<b>1</b>	Fail	Fail	0.22	0.47
29	LibNPDB202	0	Pass	Fail	0.58	0.70	68	LibNPDB352	0	Fail	Fail	0.41	0.45
30	LibNPDB243	0	Pass	Fail	0.46	0.58	69	LibNPDB353	<b>2</b>	Fail	Fail	0.11	0.48
31	LibNPDB244	0	Pass	Fail	0.45	0.70	70	LibNPDB354	0	Fail	Fail	0.41	0.43
32	LibNPDB245	0	Pass	Pass	0.51	0.51	71	LibNPDB355	<b>3</b>	Fail	Fail	0.09	0.45
33	LibNPDB246	<b>1</b>	Fail	Fail	0.23	0.46	72	LibNPDB356	<b>1</b>	Pass	Pass	0.44	0.53
34	LibNPDB247	0	Pass	Pass	0.51	0.51	73	LibNPDB357	<b>2</b>	Fail	Fail	0.28	0.41
35	LibNPDB248	0	Pass	Fail	0.72	0.60	74	LibNPDB358	<b>1</b>	Fail	Pass	0.24	0.44
36	LibNPDB249	0	Pass	Fail	0.69	0.66	75	LibNPDB359	<b>2</b>	Fail	Pass	0.28	0.63
37	LibNPDB250	0	Pass	Fail	0.79	0.53	76	LibNPDB360	0	Pass	Fail	0.46	0.56
38	LibNPDB251	0	Pass	Fail	0.61	0.53	77	LibNPDB384	0	Pass	Fail	0.61	0.61
39	LibNPDB252	<b>3</b>	Fail	Fail	0.2	0.46	78	LibNPDB400	<b>1</b>	Pass	Fail	0.34	0.44

Note: LRO5V, Lipinski's Rule of Five Violations.

### Structural Classification

Analysis of the (ArbC) library collected from literature reveals a distinct distribution of compounds across various biochemical classifications. The constituents were categorized into two biosynthetic pathways, eight superclasses, and thirty-two classes, with the data indicating a significant concentration within a few major categories. As presented in (Figure 2), the biosynthetic pathways show that a vast majority of the compounds originate from three predominant routes: shikimates and phenylpropanoids, which represent the largest group at 57.7%; and terpenoids, at 42.3%. At the superclass level, the most prominent groups are

Sesquiterpenoids (28%), Flavonoids (20%), and Phenolic acids (20%). The classification becomes more granular at the class level, where the most prevalent classes identified include cinnamic acids and derivatives (14.9%), Simple phenolic acids (12.2%), Flavonols (6.76%), and Flavan-3-ols (6.76%). This hierarchical breakdown highlights both the extensive chemical diversity of the *A. pavarii* library and the dominance of particular structural scaffolds, underscoring the plant's rich biosynthetic repertoire [13,14,19].

### Structural classification of the *Arbutus pavarii* Pamp compounds

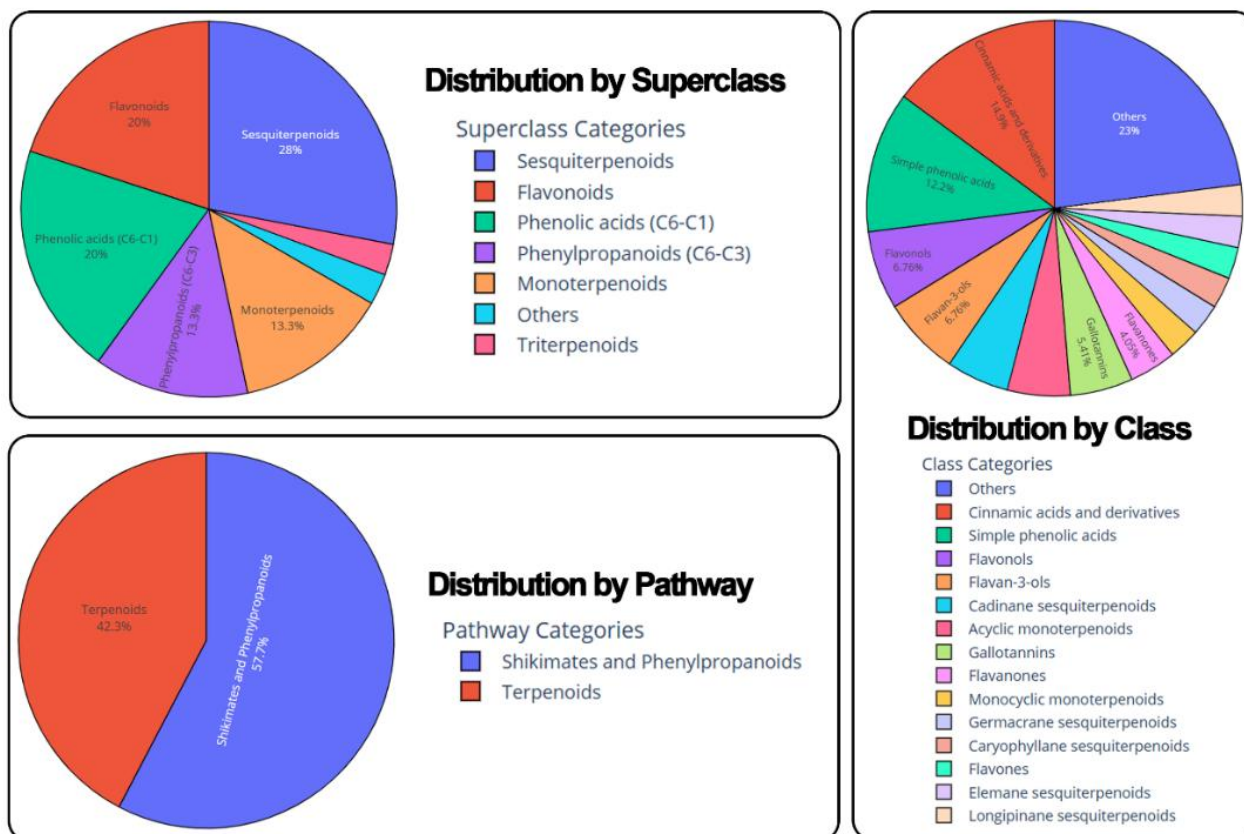


**Figure 2. Structural classification of the phytochemicals isolated from *A. pavarii*. The pie charts illustrate the distribution of compounds based on their biosynthetic pathway, chemical superclass, and specific chemical class.**

#### Validation of Molecular Docking Protocol

As shown in (Figure 3), the native co-crystallized ligand Mefenamic acid was redocked within the inhibitor binding cavity of COX-2 (PDB ID: 5IKR). The RMSD value was subsequently determined by comparing the docked pose (blue) to the crystal structure conformation (yellow). The predicted docking pose (blue) of Mefenamic acid displayed RMSD value of 0.335 Å, providing strong evidence for the reliability and reproducibility of the scoring function implemented in the MOE docking protocol, used in the current study [4-6]. The ( $\Delta G_b$ ) obtained for the redocked (Mefenamic acid) pose was -6.885 kcal/mol.

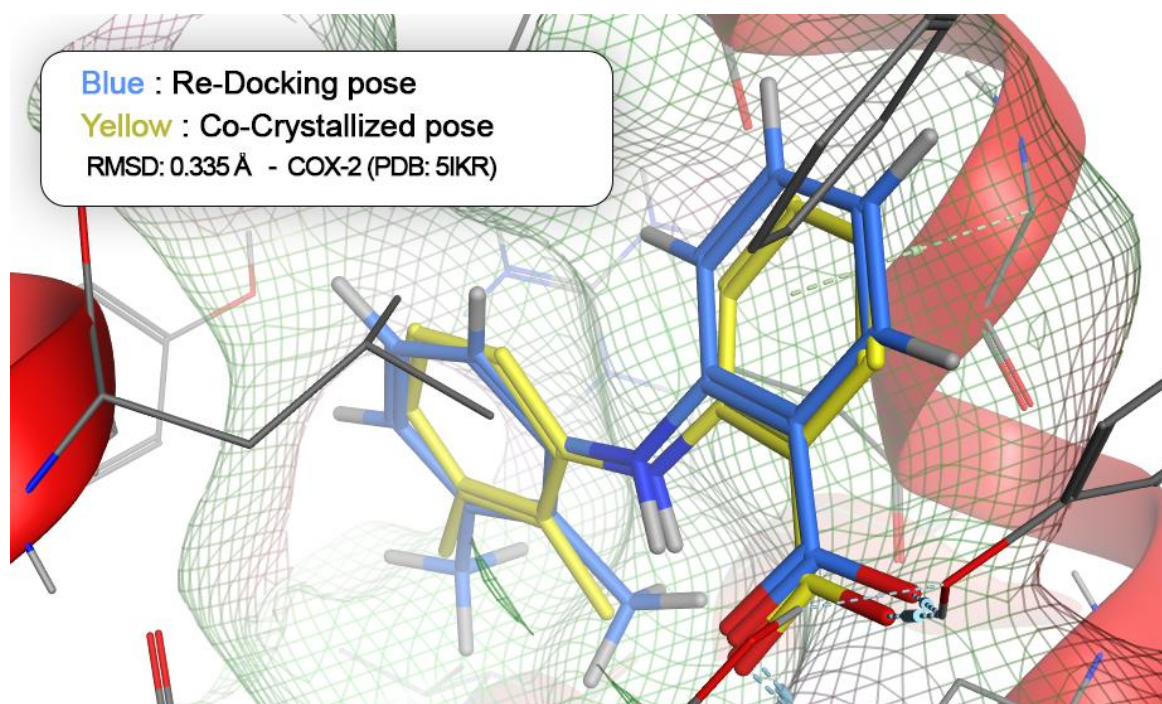


**Figure 3: Superposition of the original (yellow) and redocked (blue) poses of the native ligand mefenamic acid within the active site of COX-2 (PDB: 5IKR). The (RMSD) between the two poses is 0.335 Å. The ( $\Delta G_b$ ) obtained for the redocked pose was -6.885 kcal/mol.**

### Virtual Screening of *Arbutus pavarii* Phytochemicals

Following the validation of the docking protocol and establishing a benchmark for inhibitor potential, mefenamic acid was redocked into the active site, yielding a binding free energy ( $\Delta G_b$ ) of -6.876 kcal/mol. This value subsequently served as the reference threshold for identifying 14 promising candidates from an initial library of 78 (ArbC). For comparative context, a panel of seven NSAIDs was also docked, revealing binding free energies of -7.772, -7.101, -6.876, -6.751, -6.652, -6.636, and -5.590 kcal/mol for celecoxib, indomethacin, mefenamic acid, diclofenac, naproxen, ibuprofen, and aspirin, respectively. The primary objective was to predict their binding affinities and elucidate their potential interaction patterns. The resulting ( $\Delta G_b$ ) and specific molecular interactions for the top-performing compounds, alongside several standard (NSAIDs), are detailed in (Table 2). The simulations revealed that a subset of phytochemicals exhibited highly favorable binding energies. Notably, LibNPDB318 emerged as the most potent compound with a  $\Delta G_b$  of -8.219 kcal/mol, followed by LibNPDB350 ( $\Delta G_b$  = -7.427 kcal/mol) and LibNPDB354 ( $\Delta G_b$  = -7.165 kcal/mol). These top three compounds demonstrated stronger predicted binding affinities than the selective COX-2 inhibitor Celecoxib ( $\Delta G_b$  = -7.772 kcal/mol is an exception, but they are stronger than other NSAIDs), Indomethacin ( $\Delta G_b$  = -7.101 kcal/mol), and the native ligand Mefenamic acid ( $\Delta G_b$  = -6.876 kcal/mol). Based on this benchmark, 14 compounds exhibiting ( $\Delta G_b$ ) lower than or comparable to mefenamic acid were selected for a more detailed analysis of their interaction patterns and comparison against a panel of NSAIDs. The ( $\Delta G_b$ ) and interaction patterns of the 14 *A. pavarii* compounds were benchmarked against seven established NSAIDs.

## Discussion

### Docking Simulation Analysis

The docking results, detailed in (Table 2), reveal that several natural compounds demonstrate ( $\Delta G_b$ ) superior or comparable to these conventional drugs. The most promising candidate, LibNPDB318, exhibited a superior ( $\Delta G_b$ ) of -8.219 kcal/mol, surpassing all tested standards, including the highly selective COX-2 inhibitor Celecoxib (-7.772 kcal/mol) [4]. Following this, LibNPDB350 and LibNPDB354 also showed highly favorable ( $\Delta G_b$ ) of -7.427 kcal/mol and -7.165 kcal/mol, respectively. These values indicate a stronger binding affinity than Indomethacin (-7.101 kcal/mol), Mefenamic Acid (-6.876 kcal/mol), and Diclofenac (-6.751 kcal/mol).



**Table 2: Molecular docking result of (ArbC) and standard NSAID drugs to COX-2 (PDB: 5IKR).**

No	Compounds	$\Delta G_b^*$	N*	Interaction Type	Residues
1	Celecoxib	-7.772	6	Polar	VAL 523 (A) H-donor, HIS 90 (A) H-donor, LEU 352 (A) H-donor, PHE 518 (A) H-acceptor
				Non-polar	SER 353 (A) pi-H
2	Indomethacin	-7.101	4	Polar	ARG 120 (A) H-acceptor, ARG 120 (A) ionic, MET 522 (A) H-donor, SER 530 (A) H-acceptor
				Non-polar	-
3	Mefenamic acid (Native)	-6.876	4	Polar	TYR 385 (A) H-acceptor, SER 530 (A) H-acceptor
				Non-polar	VAL 523 (A) pi-H, GLY 526 (A) pi-H
4	Diclofenac	-6.751	2	Polar	SER 530 (A) H-acceptor
				Non-polar	GLY 526 (A) pi-H
5	Naproxen	-6.652	3	Polar	ARG 120 (A) H-acceptor, ARG 120 (A) ionic
				Non-polar	VAL 523 (A) pi-H
6	Ibuprofen	-6.636	2	Polar	ARG 120 (A) H-acceptor, ARG 120 (A) ionic
				Non-polar	-
7	Aspirin	-5.590	2	Polar	SER 530 (A) H-acceptor
				Non-polar	ALA 527 (A) pi-H
8	LibNPDB318	-8.219	5	Polar	ARG 120 (A) H-acceptor, TYR 355 (A) H-acceptor
				Non-polar	TYR 115 (A) pi-H, GLY 526 (A) pi-H, VAL 89 (A) pi-H
9	LibNPDB350	-7.427	4	Polar	SER 530 (A) H-acceptor, ARG 120 (A) H-acceptor, VAL 523 (A) H-acceptor, TYR 385 (A) H-acceptor
				Non-polar	-
10	LibNPDB354	-7.165	3	Polar	ARG 120 (A) H-acceptor, TYR 355 (A) H-acceptor
				Non-polar	ALA 527 (A) pi-H
11	LibNPDB174	-6.758	2	Polar	-
				Non-polar	ALA 527 (A) pi-H, LEU 531 (A) pi-H
12	LibNPDB250	-6.737	2	Polar	ARG 120 (A) H-acceptor
				Non-polar	ALA 527 (A) pi-H
13	LibNPDB360	-6.721	3	Polar	SER 530 (A) H-acceptor, VAL 523 (A) H-acceptor, TYR 385 (A) H-acceptor
				Non-polar	-
14	LibNPDB090	-6.609	4	Polar	ARG 120 (A) H-acceptor, ARG 120 (A) H-acceptor, SER 530 (A) H-acceptor
				Non-polar	TYR 385 (A) H-pi
15	LibNPDB247	-6.585	4	Polar	TYR 355 (A) H-donor, ALA 527 (A) H-acceptor, MET 522 (A) H-donor
				Non-polar	LEU 531 (A) pi-H
16	LibNPDB109	-6.518	3	Polar	SER 530 (A) H-acceptor
				Non-polar	ALA 527 (A) pi-H, LEU 352 (A) pi-H
17	LibNPDB103	-6.407	3	Polar	GLN 192 (A) H-donor, ALA 527 (A) H-acceptor
				Non-polar	ALA 527 (A) pi-H
18	LibNPDB256	-6.393	2	Polar	SER 530 (A) H-acceptor
				Non-polar	TYR 385 (A) H-pi
19	LibNPDB359	-6.375	3	Polar	ARG 120 (A) H-acceptor
				Non-polar	SER 353 (A) pi-H, GLY 526 (A) pi-H
20	LibNPDB187	-6.280	4	Polar	SER 530 (A) H-acceptor
				Non-polar	ALA 527 (A) pi-H
21	LibNPDB080	-6.155	3	Polar	VAL 523 (A) H-acceptor
				Non-polar	ALA 527 (A) pi-H

**Note:** ( $\Delta G_b$ )- Binding Energy, (N) Number of interactions.

Notably, a significant number of compounds displayed binding affinities that were highly competitive with widely used NSAIDs. The ( $\Delta G_b$ ) for LibNPDB174 (-6.758 kcal/mol), LibNPDB250 (-6.737 kcal/mol), and LibNPDB360 (-6.721 kcal/mol) were nearly identical to that of Diclofenac (-6.751 kcal/mol). Similarly, LibNPDB090 (-6.609 kcal/mol) demonstrated a binding affinity comparable to that of Naproxen (-6.652 kcal/mol) and Ibuprofen (-6.636 kcal/mol). The remaining lead compounds, while exhibiting lower potency than most standards, still presented more favorable ( $\Delta G_b$ ) than Aspirin (-5.590 kcal/mol), suggesting they possess relevant inhibitory potential [17,26].

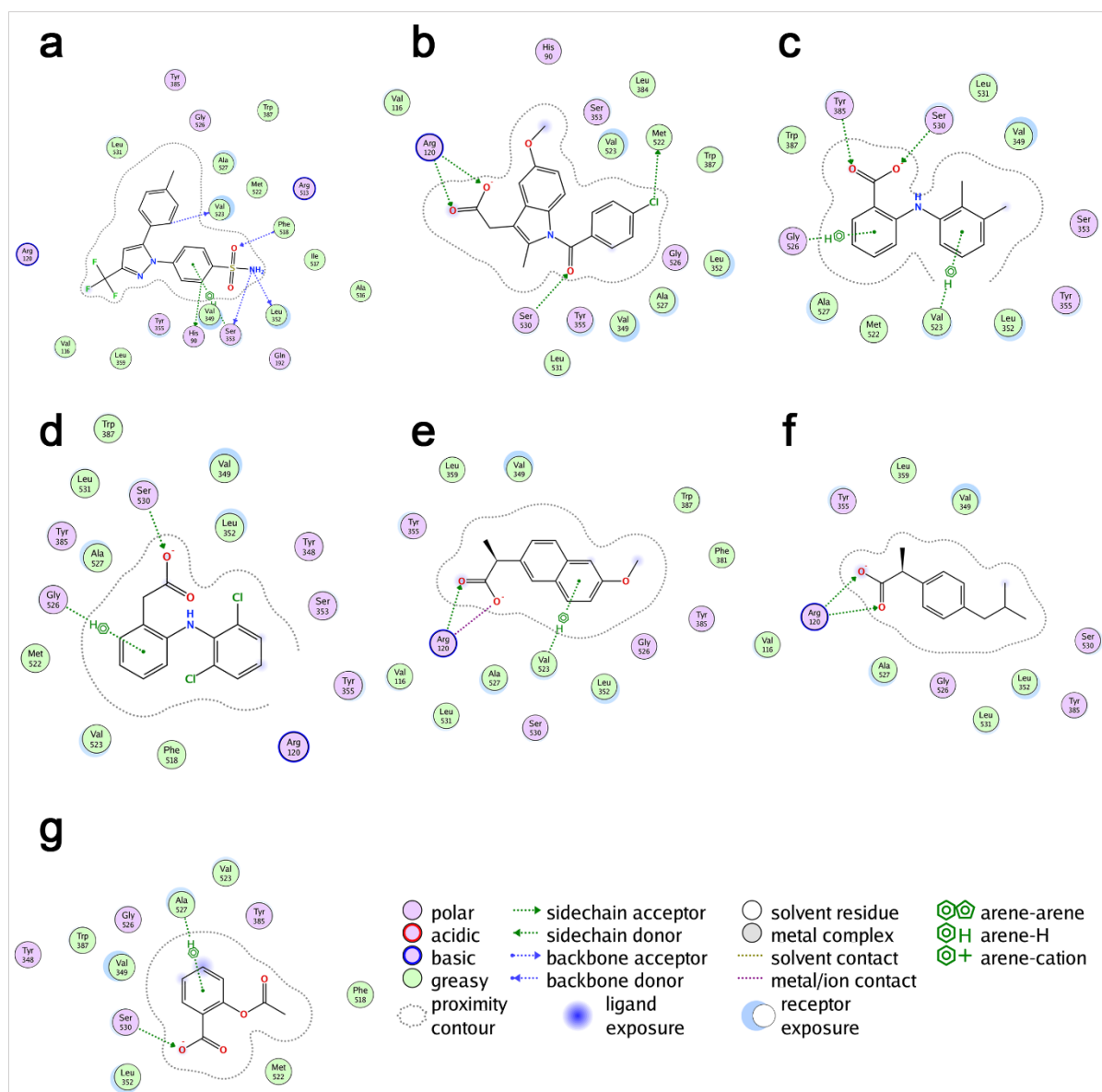


**Figure 4. 2D interaction diagrams of standard NSAIDs docked into the active site of COX-2 (PDB ID: 5IKR). The panels show the binding interaction for: (a) Celecoxib, (b) Indomethacin, (c) Mefenamic-acid, (d) Diclofenac, (e) Naproxen, (f) Ibuprofen and (g) Aspirin. The legend indicates the types of amino acid residues and the nature of the molecular interactions shown.**

A detailed analysis of the ligand receptor interactions reveals that the lead compounds from *A. pavarii* engage the COX-2 active site through binding modalities analogous to those of established NSAIDs. The COX-2 active site is primarily characterized by two key regions that govern inhibitor binding: a construction site formed by Arg-120 and Tyr-355, and a catalytic apex involving Tyr-385 and Ser-530 [3]. Several of the most potent compounds anchor themselves at the entrance of the active site channel, a mechanism characteristic of traditional "profens". LibNPDB318 (-8.219 kcal/mol), the top-scoring compound, forms a crucial hydrogen bond with the gatekeeper residue Arg-120 [27]. This interaction is also leveraged by LibNPDB354, LibNPDB250, and LibNPDB359. Notably, LibNPDB090 mimics the binding signature of Naproxen and Ibuprofen by forming two hydrogen bonds with Arg-120 and an additional contact with Ser-530, effectively occluding the substrate channel.

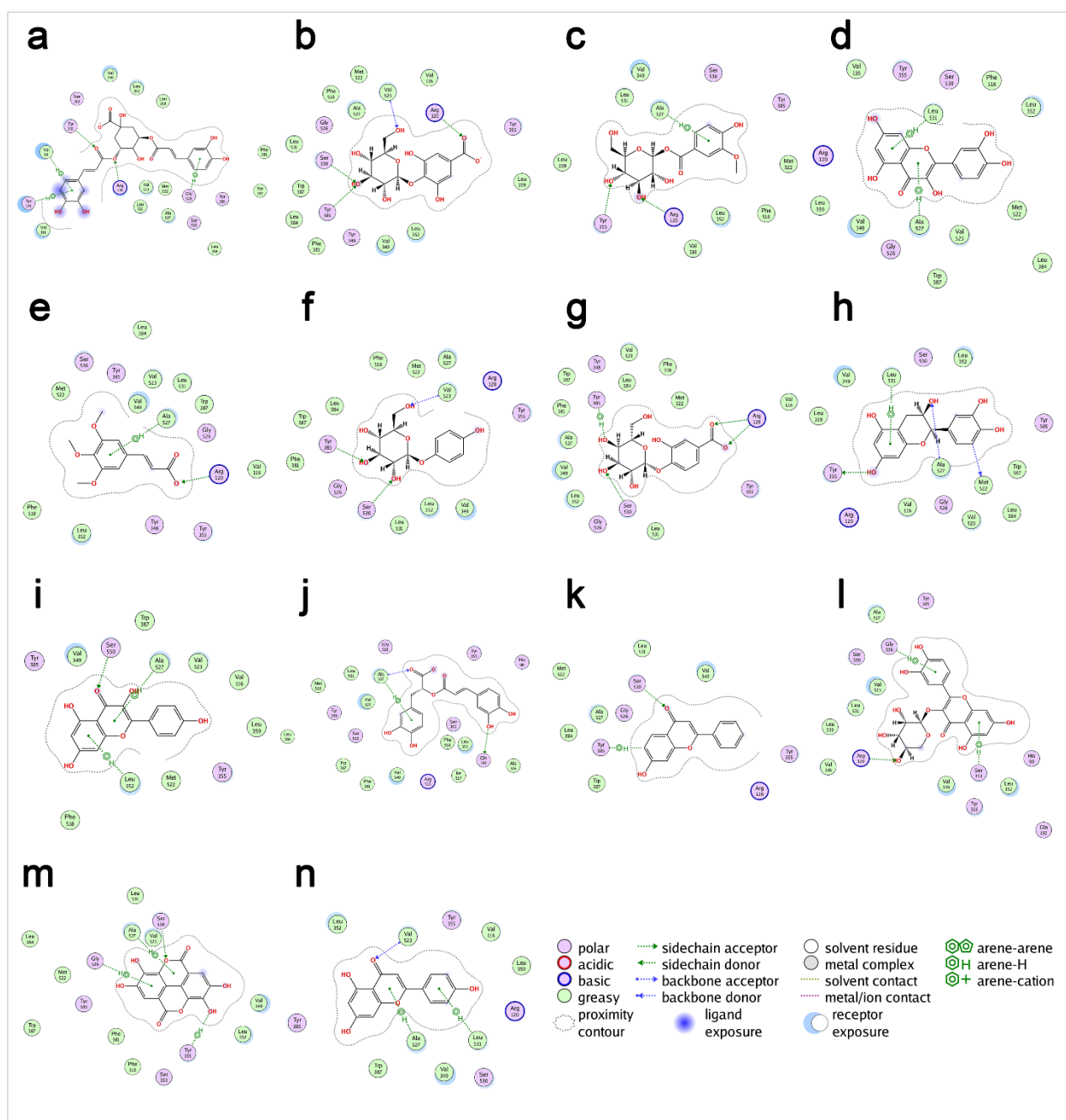


**Figure 5.** 2D interaction diagrams of the top ranking (ArbC) docked into the active site of COX-2 (PDB ID: 5IKR). The panels show the binding modes for: (a) LibNPDB318, (b) LibNPDB350, (c) LibNPDB354, (d) LibNPDB174, (e) LibNPDB250, (f) LibNPDB360, (g) LibNPDB090, (h) LibNPDB247, (i) LibNPDB109, (j) LibNPDB103, (k) LibNPDB256, (l) LibNPDB359, (m) LibNPDB187, and (n) LibNPDB080. The legend indicates the amino acid residues and the nature of the molecular interactions.

In contrast, LibNPDB360 and LibNPDB256 adopt an "inverted" binding pose, a mode first characterized for Diclofenac. These compounds bypass the Arg-120 gatekeeper and interact directly with residues at the catalytic apex, with LibNPDB360 forming polar contacts with both Tyr-385 and Ser-530. This binding orientation is mechanistically significant, as inhibitors of this class often retain potency against Arg-120 mutations [3,27]. Perhaps most impressively, LibNPDB350 demonstrates a sophisticated hybrid binding mechanism. With a strong ( $\Delta G_b$ ) of -7.427 kcal/mol, it simultaneously engages residues at both the canonical (Arg-120) and inverted (Ser-530, Tyr-385) binding sites, an interaction network reminiscent of oxicam class inhibitors. Its additional polar interaction with Val-523, a residue bordering the COX-2 selective side pocket, also suggests a potential for selective inhibition. Furthermore, the remarkable mimicry of LibNPDB187, which exhibits an interaction pattern identical to Aspirin by forming a hydrogen bond with the critical Ser-530 residue, provides strong evidence for its potential as a competitive COX-2 inhibitor [3,17,26,27].

Beyond these favorable binding interactions, the chemoinformatic analysis revealed that numerous compounds from the *A. pavarii* library also exhibit exceptional drug-like properties. For example, LibNPDB255 displayed zero Lipinski violations, a high QED score of 0.79, and a minimal predicted toxicity score of 0.43. Similarly, LibNPDB080, LibNPDB250, and LibNPDB256 achieved zero Lipinski violations with impressive QED scores of 0.63, 0.79, and 0.71, respectively. This convergence of potent inhibitory activity and favorable molecular properties suggests their capacity to perform as well as synthetic NSAIDs, while potentially offering improved safety profiles [24,25]. The inherent structural diversity within the library provides a strategic advantage for hit-to-lead optimization. Consequently, the top compounds are positioned as promising scaffolds for the development of novel analgesic and anti-inflammatory agents.

Ultimately, while this computational evidence positions *A. pavarii* as a valuable resource for medicinal chemistry, it necessitates empirical validation. The following essential phase in transferring these promising *in-silico* predictions into practical treatment alternatives is experimental confirmation of their anti-inflammatory efficacy, which is limited by their inherent limitations. The docking calculations represent idealized binding scenarios that do not fully account for protein flexibility, solvation effects, or the allosteric considerations that influence biological activity. Additionally, the current analysis focuses exclusively on binding affinity without considering critical factors such as COX-1/COX-2 selectivity ratios, which are essential for developing safer NSAID therapies. Nevertheless, these *in-silico* findings, corroborated by traditional use and existing *in-vitro* data, strongly support further investigation into the anti-inflammatory potential of *A. pavarii*. Priority should be given to compounds with the most favorable binding energies for progression into enzymatic and cell-based assays, as well as more advanced computational and *in vivo* studies.

## Conclusion

This study successfully bridged the gap between the traditional use of *Arbutus pavarii* and modern computational drug discovery. By systematically collecting and performing chemoinformatic analysis on 78 of its phytochemicals, this work has also significantly enriched the Libyan Natural Products Database (LibNPDB), which is freely accessible to the scientific community at <https://www.libnpdb.ly/libnpdb-search>. The molecular docking simulations against the COX-2 enzyme provided a robust molecular rationale for the plant's traditionally recognized anti-inflammatory and analgesic properties. Our findings revealed that several compounds within *A. Pavarii* possess predicted binding affinities comparable or superior to established NSAIDs, engaging the enzyme's active site through diverse and sophisticated mechanisms. Consequently, this work validates the therapeutic potential of *A. pavarii* at a molecular level and identifies its constituent phytochemicals as a rich reservoir of promising scaffolds for the development of novel analgesic and anti-inflammatory agents.

## Conflicts of Interest

The authors declare no conflicts of interest.

## References

1. Gurib-Fakim A. Medicinal plants: Traditions of yesterday and drugs of tomorrow. *Mol Aspects Med.* 2006 Feb;27(1):1-93. doi: 10.1016/j.mam.2005.07.008. PMID: 16105678.
2. Cheuka P, Mayoka G, Mutai P, Chibale K. The Role of Natural Products in Drug Discovery and Development against Neglected Tropical Diseases. *Molecules.* 2016 Dec 31;22(1):58. doi: 10.3390/molecules22010058. PMID: 28042865; PMCID: PMC6155950.
3. Rowlinson SW, Kiefer JR, Prusakiewicz JJ, Pawlitz JL, Kozak KR, Kalgutkar AS, et al. A novel mechanism of cyclooxygenase-2 inhibition involving interactions with Ser-530 and Tyr-385. *J Biol Chem.* 2003 Nov 14;278(46):45763-9. doi: 10.1074/jbc.M305481200. PMID: 12960163.
4. Sasi A, Abu-Fanas H, Al-Shawin K, Ataalib S. Investigation of the Analgesic and Anti-Inflammatory Potential of *Moringa oleifera*: Molecular Docking Analysis. *Libyan J Med Appl Sci.* 2025 Jul;3(3):26-35. doi: <https://ljmas.com/index.php/journal/article/view/111>.
5. Obikeze K, Sasi AA, Raji I. In-silico and in-vivo evaluation of the Cardiovascular effects of five *Leonotis leonurus* diterpenes. *Sci Afr.* 2023 Mar;19:e01510. doi: 10.1016/j.sciaf.2022.e01510.
6. Abd-Elhakim YM, et al. Investigation of the In-Vivo Cytotoxicity and the In Silico-Prediction of MDM2-p53 Inhibitor Potential of *Euphorbia peplus* Methanolic Extract in Rats. *Toxins (Basel).* 2019 Nov 1;11(11):642. doi: 10.3390/toxins11110642. PMID: 31683851; PMCID: PMC6891739.
7. Sasi A, Rafieda A, Jouda S, Yacoub A, Khalifa F. Bridging the gap: A strategic review of natural product databases and the proposal for the Libyan Natural Products Database (LibNPDB). *Mediterr J Pharm Pharm Sci.* 2025 Jul;5(3):38-45. doi: <https://doi.org/10.5281/zenodo.16334228>.
8. Hebail F, Rahouma K, Muftah A, Aldroujee A, Elghmasi S. Estimating Antioxidant and Free Radical Scavenging Activity of *Arbutus Pavarii* Extracts. *AlQalam J Med Appl Sci.* 2024 Mar:65-73.
9. Geroushi AAG. *Arbutus pavarii* Pamp. - An updated profile. *Trends Phytochem Res.* 2021 Jan [cited 2022 Oct 21]. Available from: [https://www.academia.edu/59486407/Arbutus\\_pavarii\\_Pamp\\_An\\_updated\\_profile](https://www.academia.edu/59486407/Arbutus_pavarii_Pamp_An_updated_profile)
10. Elside M, Elmghirbi W, Alghros M, Benelhaj K. Antilithiatic Activity of *Arbutus Pavarii* (Shemeri) Extract on Ethylene Glycol Induced Lithiasis in Rats. *Khalij-Libya J Dent Med Res.* 2023 Dec:129-136. doi: 10.47705/kjdmr.2370210.



11. Alghazeer R, et al. Investigation of the potential anti-fertility activity of *Arbutus pavarii* in male mice. *Acta Pol Pharm*. 2020 Dec;77(5):725-35. doi: 10.32383/appdr/127965.
12. Shatshat SE, Elshibani F. Characteristics, nutritive value and antioxidant content of the Libyan endemic (*Arbutus pavarii* Pamp.) strawberry tree fruits. *EPRA Int J Res Dev (IJRD)*. 2020 Sep;5(9).
13. Elshibani FA, et al. A multidisciplinary approach to the antioxidant and hepatoprotective activities of *Arbutus pavarii* Pampan fruit; in vitro and in vivo biological evaluations, and in silico investigations. *J Enzyme Inhib Med Chem*. 2024 Dec;39(1):2293639. doi: 10.1080/14756366.2023.2293639.
14. Alsabri S, et al. Phytochemical screening, antioxidant, antimicrobial and anti-proliferative activities study of *Arbutus pavarii* plant. *J Chem Pharm Res*. 2013 Jan;5:32-6.
15. Vivek-Ananth RP, Mohanraj K, Sahoo AK, Samal A. IMPPAT 2.0: An Enhanced and Expanded Phytochemical Atlas of Indian Medicinal Plants. *ACS Omega*. 2023 Mar 7;8(9):8827-45. doi: 10.1021/acsomega.3c00156. PMID: 36910987; PMCID: PMC10004688.
16. Sinha S, Hazarika A, Johari S, Neog B, Rajkhowa S, Biswas A. IMPDB: Indian Medicinal Phytochemical Database Curated for Drug Designing. *J Comput Biophys Chem*. 2022 Sep;21(6):709-28. doi: 10.1142/S2737416522500302.
17. Nayak A, et al. Exploring molecular docking with MM-GBSA and molecular dynamics simulation to predict potent inhibitors of cyclooxygenase (COX-2) enzyme from terpenoid-based active principles of *Zingiber* species. *J Biomol Struct Dyn*. 2023 Dec;41(20):10840-50. doi: 10.1080/07391102.2022.2161011. PMID: 36571360.
18. Pu L, Naderi M, Liu T, Wu HC, Mukhopadhyay S, Brylinski M. eToxPred: a machine learning-based approach to estimate the toxicity of drug candidates. *BMC Pharmacol Toxicol*. 2019 Jan 7;20(1):2. doi: 10.1186/s40360-018-0282-6. PMID: 30616631; PMCID: PMC6323713.
19. Kim HW, et al. NPClassifier: A Deep Neural Network-Based Structural Classification Tool for Natural Products. *J Nat Prod*. 2021 Nov 26;84(11):2795-807. doi: 10.1021/acs.jnatprod.1c00399. PMID: 34757796; PMCID: PMC8625029.
20. Sorokina M, Merseburger P, Rajan K, Yirik MA, Steinbeck C. COCONUT online: Collection of Open Natural Products database. *J Cheminform*. 2021 Jan 7;13(1):2. doi: 10.1186/s13321-020-00478-9. PMID: 33415543; PMCID: PMC7792598.
21. Barazorda-Ccahuana HL, et al. PeruNPDB: the Peruvian Natural Products Database for in silico drug screening. *Sci Rep*. 2023 May 9;13(1):7577. doi: 10.1038/s41598-023-34729-0. PMID: 37161039; PMCID: PMC10170670.
22. Isa MA, et al. In silico molecular docking and molecular dynamic simulation of potential inhibitors of 3C-like main proteinase (3CLpro) from severe acute respiratory syndrome coronavirus-2 (SARS-CoV-2) using selected african medicinal plants. *Adv Tradit Med*. 2022 Mar;22(1):107-23. doi: 10.1007/s13596-020-00523-w. PMID: 33192217; PMCID: PMC7657215.
23. Rutz A, et al. The LOTUS Initiative for Open Natural Products Research: Knowledge Management through Wikidata. *bioRxiv [Preprint]*. 2021 Dec 1:2021.02.28.433265. doi: 10.1101/2021.02.28.433265. PMID: 33688656; PMCID: PMC7941628.
24. Gómez-García A, et al. Updating and profiling the natural product-likeness of Latin American compound libraries. *Mol Inform*. 2024 Jul;43(7):e202400052. doi: 10.1002/minf.202400052.
25. Bickerton GR, Paolini GV, Besnard J, Muresan S, Hopkins AL. Quantifying the chemical beauty of drugs. *Nat Chem*. 2012 Feb;4(2):90-8. doi: 10.1038/nchem.1243. PMID: 22270643.
26. Utami W, Aziz HA, Fitriani IN, Zikri AT, Mayasri A, Nasrudin D. In silico anti-inflammatory activity evaluation of some bioactive compound from *figus religiosa* through molecular docking approach. *J Phys Conf Ser*. 2020 Jun;1563(1):012024. doi: 10.1088/1742-6596/1563/1/012024.
27. Xu S, et al. Oxicams bind in a novel mode to the cyclooxygenase active site via a two-water-mediated H-bonding network. *J Biol Chem*. 2014 Mar 7;289(10):6799-808. doi: 10.1074/jbc.M113.517987. PMID: 24403070; PMCID: PMC3945364.